Article

J. Mex. Chem. Soc. **2025**, *69*(3)
Regular Issue

ISSN-e 2594-0317

^{1}H NMR-based Chemical Profiling of Retail Samples of *Peumus boldus* (Boldo) Leaves

Estefanía de Jesús Terán-Sánchez[1], Yair Cruz-Narvaez[3], Erick Alejandro Herrera-Jurado[1], Mabel M. Montenegro-Sustaita[1], Elvia Becerra-Martínez[2*], L. Gerardo Zepeda-Vallejo[1*]

[1]Departamento de Química Orgánica, Escuela Nacional de Ciencias Biológicas, Instituto Politécnico Nacional, Av. Prolongación de Carpio y Plan de Ayala s/n, Col. Santo Tomás, Delegación Miguel Hidalgo, Ciudad de Mexico 11340, Mexico.
[2]Centro de Nanociencias y Micro y Nanotecnologías, Instituto Politécnico Nacional, Av. Luis Enrique Erro S/N, Unidad Profesional Adolfo López Mateos, Zacatenco, Delegación Gustavo A. Madero, Ciudad de México, 07738, México.
[3]Escuela Superior de Ingeniería Química e Industrias Extractivas, Instituto Politécnico Nacional, Av. Luis Enrique Erro S/N, Unidad Profesional Adolfo López Mateos, Zacatenco, Delegación Gustavo A. Madero, Ciudad de México, 07738, México.

***Corresponding author:** Elvia Becerra-Martínez, email: elmartinezb@ipn.mx; L. Gerardo Zepeda-Vallejo, email: lzepeda@ipn.mx

Received July 15th, 2024; Accepted September 18th, 2024.

DOI: http://dx.doi.org/10.29356/jmcs.v69i3.2336

This research is dedicated to the distinguished academic career of Dr. Joaquín Tamariz Mascarúa

Abstract. Aqueous extracts of seven commercial samples of boldo leaves (*Peumus boldus*) were subjected to ^{1}H NMR analysis to elucidate their chemical profiling. The ground leaves were extracted with ultrasound using water as a solvent at 60 °C for 15 min. The resulting extracts were then analyzed using ^{1}H NMR spectroscopy, unveiling the presence of seven amino acids (alanine, asparagine, glutamine, phenylalanine, proline, tyrosine, and valine), three sugars (α- and β-glucose, fructose, and sucrose), and seven short-chain carboxylic acids (acetic, citric, formic, glyceric, malic, malonic, and succinic acids). Through multivariate statistical analysis of the gathered ^{1}H NMR data, including PCA and OPLS-DA, a consistent chemical profile emerged across the examined samples. Variations were mainly due to differences in the relative concentrations of the mentioned metabolites. In addition, High Resolution Mass Spectrometry-ESI (HRMS-ESI) confirmed the presence of boldine in all samples tested, aiding in the authentication of boldo samples. Additionally, the major alkaloid N-methyllaurotetanine, a typical component of boldo leaves, was also identified.
Keywords: ^{1}H NMR; *Peumus boldus* M.; aqueous extract; chemical profiling; multivariate analysis; HRMS-ESI; boldine.

Resumen. Los extractos acuosos de siete muestras comerciales de hojas de boldo (*Peumus boldus*) se sometieron a análisis de RMN ^{1}H para dilucidar su perfil químico. Las hojas molidas se extrajeron por ultrasonido utilizando agua como disolvente a 60°C durante 15 minutos. Los extractos resultantes se sometieron a análisis por RMN ^{1}H, revelando la presencia de siete aminoácidos (alanina, asparagina, glutamina, fenilalanina, prolina, tirosina y valina), tres azúcares (α y β-glucosa, fructosa y sacarosa) y siete ácidos carboxílicos de cadena corta (acético, cítrico, glicérico, málico, malónico y succínico). Mediante el análisis estadístico multivariante de los datos de RMN ^{1}H reunidos, incluyendo PCA y OPLS-DA, se observó un perfil químico coherente en todas las muestras

J. Mex. Chem. Soc. **2025**, *69*(3)
Regular Issue

ISSN-e 2594-0317

examinadas. Las variaciones se debieron principalmente a diferencias en las concentraciones relativas de los metabolitos mencionados. Además, la espectrometría de masas de alta resolución-ESI (HRMS-ESI) confirmó la presencia de boldina en todas las muestras analizadas, ayudando a la autenticación de las muestras de boldo. También se identificó el alcaloide principal *N*-metillaurotetanina, un componente típico de las hojas de boldo.
Palabras clave: RMN ^{1}H; *Peumus boldus* M.; extracto acuoso; perfil químico; análisis multivariante; HRMS-ESI.

Introduction

Peumus boldus, commonly referred to as boldo, is a small tree native from Chile and Peru. Belonging to the Monimiaceae family, it is esteemed for its fragrant leaves, which have been employed as a culinary spice for centuries [1]. The leaves of boldo are frequently infused for their medicinal attributes [2]. Traditionally, they have been used to alleviate a spectrum of digestive complaints, including indigestion [3], constipation, and flatulence [4]. Boldo is also recognized for its diuretic properties [5] and its potential to safeguard liver health [6].

Peumus boldus, or boldo, harbors a diverse array of metabolites, encompassing alkaloids, flavonoids, terpenoids, and various other compounds. Among these constituents, boldine and isoboldine stand out as the primary alkaloids in boldo leaves. Boldine is renowned for its diversity of properties, including antioxidant [7], anti-inflammatory [8], and hepatoprotective [9] attributes. It has been extensively studied for its potential in treating liver diseases, such as hepatitis and cirrhosis [10]. Isoboldine, a positional isomer of boldine, has exhibited anti-feeding effects [11]. *Peumus boldus* is rich in flavonoids, including quercetin, isorhamnetin, and kaempferol glycosides, known for their antioxidant and anti-inflammatory properties. These compounds have been explored for their potential in the management of cancer and cardiovascular diseases [12]. Additionally, *Peumus boldus* contains diverse terpenoids, such as piperitone oxide, α-terpinene, eucalyptol [13], and ascaridole [14], which have demonstrated antifungal and larvicidal activities. While *Peumus boldus* has been extensively researched for its potential health benefits, particularly in the treatment of liver and digestive conditions, it is imperative to broaden the scope of such investigations to comprehensively elucidate the pharmacological properties and ensure the safety of consuming this medicinal plant.

Currently, *Peumus boldus* is in high commercial demand due to its highly praised medicinal properties. Therefore, rigorous quality control measures are essential to ensure both its authenticity and safety for consumption. Various validation and authenticity methods for *Peumus boldus* have been devised, primarily relying on trichome micromorphology [15], HPLC [16], UPLC-QTOF-MS [17], or botanical profiling [18]. Chemical profiling is a highly effective and widely used approach for establishing authenticity criteria in medicinal plants. In particular, NMR stands out as one of the most reliable analytical platforms for performing this task. In this context, numerous authors have detailed the chemical profiling of *Peumus boldus*, using ^{13}C NMR [19], MS-based [20] techniques, or comprehensive protocols incorporating both analytical platforms [21]. To the best of our knowledge, a ^{1}H NMR-based metabolomic profiling of *Peumus boldus* has not been documented. This prompted our efforts to establish such a profiling through a simple and reproducible protocol, intended for use as a benchmark for quality control and authentication of commercial samples. To achieve this objective, aqueous extracts of seven commercially available boldo samples were used, closely replicating the traditional infusion prepared for consumption.

In addition, High-Resolution Mass Spectrometry Electrospray Ionization (HRMS-ESI) was employed to validate the presence of boldine in the aqueous extracts, as this alkaloid serves as a key authenticity marker for boldo.

Experimental

Source of retail samples and preparation of extracts

The seven boldo samples were sourced from various natural stores within the "Central de Abastos" of Mexico City, as well as online providers. Prior to analysis, rigorous cleaning was carried out, with only leaves

J. Mex. Chem. Soc. **2025**, *69*(3)
Regular Issue

ISSN-e 2594-0317

of uniform appearance and optimal preservation being chosen. Any residual flowers, twigs, or leaves displaying dissimilar characteristics were excluded and analyzed separately. The selected leaves were then finely ground to achieve a consistent particle size (1-4 mm). Subsequently, 4 g of each sample was treated with 25 mL of hot water (80 °C) and allowed to steep for 5 minutes. Following this, the resulting suspension underwent a 15-minute sonication at 60 °C, followed by decantation and filtration through a cotton filter, and centrifugation at 10,500 rpm for 20 minutes. Finally, the supernatant was filtered through a 0.22 µm hydrophilic filter. For each sample, this process was repeated ten times.

Sample preparation for NMR analysis

To prepare the samples for NMR analysis, a 400 µL aliquot of infusion was poured into an NMR tube, followed by 140 µL of phosphate buffer at pH 5 enriched with 1 % sodium azide, and 60 µL of a 10 mM TSP standard solution in D_2O. NMR analysis of each brand of boldo tea was performed by ten replicates. A concentration of 1 mM EDTA was added to the samples to observe with better resolution the signals corresponding to citric, formic, malic and succinic acid compared to aqueous extracts without EDTA.

^{1}H NMR analysis

The ^{1}H NMR spectra used for statistical analysis were obtained at 298 K in a Bruker Avance III 750 MHz (17.6 T) spectrometer (Bruker Biospin, Rheinstetten, Germany) equipped with a 5 mm TXI probehead (PA TXI 750S4 H-C/N-D-05 Z) able to perform z-gradient. The following acquisition parameters were used: 4 dummy scans, 256 scans, FID size 64 K, pulse width 8 ms, spectral width 15 ppm, receiver gain 37.9, acquisition time 2.18 s, relaxation delay 5 s and digital resolution 0.46 Hz. For aqueous extracts, ^{1}H NMR spectra were acquired using the NOESYPR1D pulse sequence to suppress the residual signal of water. Spectra for quantification were acquired at 298 K in a Bruker Avance III 600 MHz (14.1 T) equipped with a 5 mm BBO probehead (PA BBO 600S3 BBF-H-D-05 Z SP) able to perform z-gradient: 4 dummy scans prior to 256 scans, FID size 64 K, spectral width 13,000 Hz, receiver gain 189.9, acquisition time 1.70 s, relaxation delay 5 s, and digital resolution 0.58 Hz.

Analysis by HR-MS-ESI

High-resolution mass spectra were acquired on a Bruker solariX Ion Cyclotron Resonance Fourier Transform Mass Spectrometer (Bruker Daltonics GmbH, Bremen, Germany) equipped with a 7 Tesla superconducting magnet (Magnex Scientific Inc., Yarton, GB) and an APOLO II ESI source (Bruker Daltonics GmbH, Bremen, Germany) operated in negative/positive ionization mode. The FTICR spectra were exported to peak lists with a cut-off of signal-to-noise ratio (S/N) of 6 using the DataAnalysis 5.2 software. Ions were measured in the ICR cell from m/z 43 to 3000.00 using the broadband detection mode with 2 M data points. Precursor ions were excluded after one MS/MS spectrum and released after 0.5 min. The equipment was calibrated according to the mass of boldine, favoring the formation of its molecular ion in the rest of the samples.

Identification and quantification of metabolites

The chemical profiling of boldo was determined by consulting databases such as Chenomx (Chenomx NMR Suite 8.0, Chenomx Inc., Edmonton, Alberta, Canada) (Fig. S1), HMDB (The Human Metabolome Database), PubChem and BMRB (Biological Magnetic Resonance Bank). Identification of metabolites was also supported by performing 2D NMR experiments such as ^{1}H-^{1}H COSY, HSQC, J-res and TOCSY.

Metabolite quantification from the metabolome was performed using Chenomx software, referencing the concentration of TSP at 1 mM. Metabolites were quantified at pH 5±0.5, only those that did not show overlapping signals with those of other metabolites. Quantification of metabolites was subjected to analysis of variance and Tukey's test using InfoStat software (v2008).

Pre-processing of the ^{1}H NMR spectra

The ^{1}H NMR spectra were baseline corrected, phased, referenced and normalized to the TSP signal (δ 0.0). A 0.30 Hz exponential apodization and Whittaker smoothing were performed with MestReNova

J. Mex. Chem. Soc. **2025**, *69*(3)
Regular Issue

ISSN-e 2594-0317

software (v14.2.0-26256; MestReC, Santiago de Compostela, Spain). Integral of the full spectrum was normalized to the TSP signal. All ^{1}H NMR spectra were stacked, and the binning size was set to 0.04 ppm.

Multivariate statistical analysis

Multivariate data analysis was performed with SIMCA software (v14.1 Umetrics, Sweden). Principal Component Analysis (PCA), Least Squares Regression (PLS) and Orthogonal Partial Least Squares Discriminant (OPLS-DA) were performed using the binning results from MestReNova. This facilitated the discernment of variations between the different samples. A second statistical analysis, scaled with Pareto, was performed using the concentration data obtained with the Chenomx software, which allowed to observe the relationship between metabolites and their presence or absence in each boldo leaf sample. The PLS and OPLS-DA models were validated by permutation analysis, while the discriminating metabolites were identified by their VIP value ($-1 \leq$ VIP ≥ 1). S-Plot and B-Plot Figures were constructed by considering their p(corr) values ($-0.5 \leq$ p(corr) ≥ 0.05). A third statistical analysis was performed comparing the two most different samples with each other. The statistical analysis performed at 600 MHz on the entire metabolome revealed a consistent trend compared to the analysis conducted on the 750 MHz equipment. This consistency indicates the reproducibility of the findings, irrespective of the magnetic field used (Fig. S2).

Results and discussion

The process encompasses the initial steps of botanical material preparation, extract acquisition, and sample preparation for NMR analysis, involving centrifugation, filtration, pH adjustment, and the addition of TSP in deuterium oxide. This is followed by the acquisition of ^{1}H NMR spectra and statistical analysis. Fig. 1 shows the stacked spectra of the seven samples analyzed. At first glance, a high degree of consistency in the corresponding spectra can be observed, indicating a similar chemical composition of the samples despite the fact that they were obtained from different commercial sources.

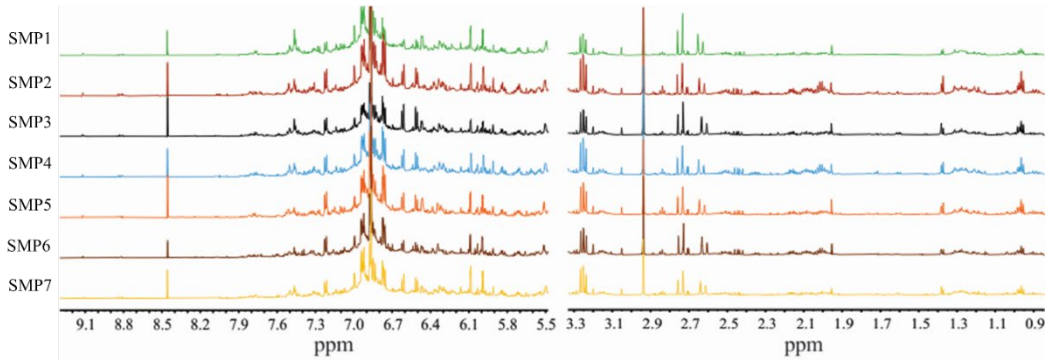

Fig. 1. Stacked ^{1}H NMR spectra (600 MHz) of the seven boldo tea samples analyzed, dopped with EDTA. For simplicity, the presaturation and sugar signals region were omitted.

A composite sample was prepared by combining equal portions of each of the seven individual samples to facilitate the identification of metabolites. Fig. 2 illustrates the resulting spectrum from the sample pool, featuring the most prominent signals of the identified metabolites. This analysis revealed a total of 17 identified metabolites, comprising seven amino acids (alanine, asparagine, glutamine, phenylalanine, proline, tyrosine, and valine), three sugars (α and β-glucose, fructose, and sucrose), and seven short-chain carboxylic acids (acetic, citric, formic, glyceric, malic, malonic, and succinic acids). Detailed information, including the names, chemical structures, and NMR parameters that facilitate identification of these metabolites, is provided in Table 1.

J. Mex. Chem. Soc. **2025**, *69*(3)
Regular Issue

ISSN-e 2594-0317

In the Experimental Section, it was observed that the commercial samples not only comprised whole leaves but also included residues of twigs and fragmented leaves of questionable authenticity. Consequently, the visually and uniform whole leaves were separated from these remains for individual analysis. The results revealed three distinct spectra, depicted in Fig. 3, revealing substantial variations in their chemical compositions. The infusion containing only boldo twigs (Fig. 3, top) exhibited decreased levels of glutamine, citric acid, and malic acid, and was notably deficient in alanine, tyrosine, aspartic acid and phenylalanine. In contrast, the spectrum of the mixture comprising finely ground twig remnants and broken leaves (Fig. 3, middle) retained the metabolite profile of twigs but displayed lower metabolite concentrations, similar to that of whole leaves (Fig. 3, bottom). Significant reductions were noted in phenylalanine (4), tyrosine (6), succinic acid (14), malic acid (12) and glutamine (3). This underscores the importance of acquiring commercial samples that preserve a considerable number of intact leaves.

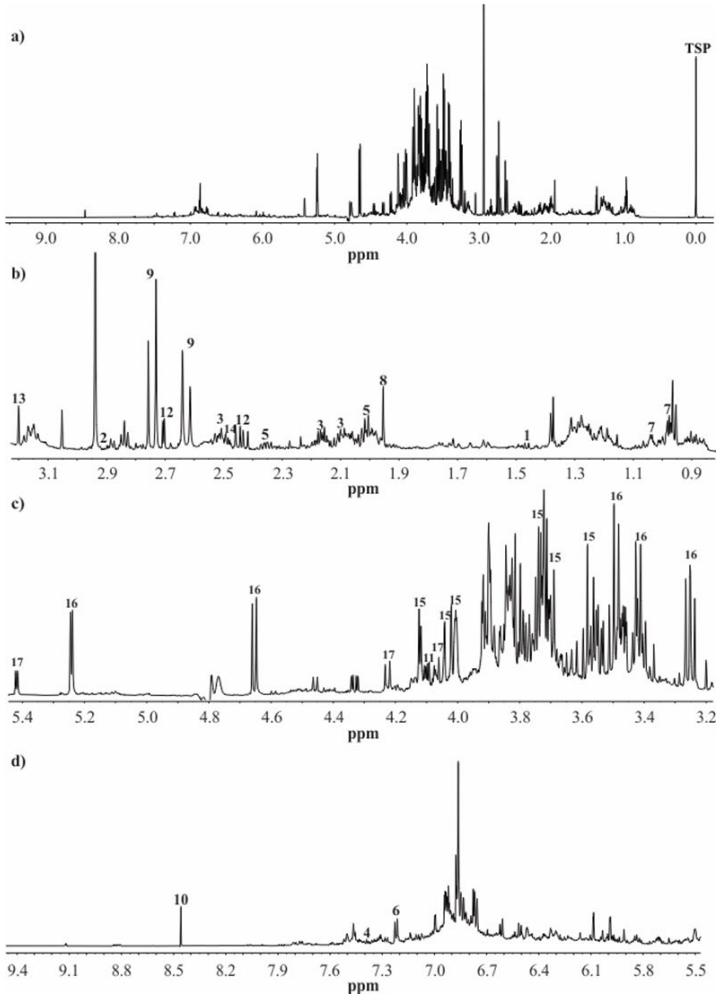

Fig. 2. ^{1}H NMR spectrum (600 MHz) of the aqueous extract of boldo with EDTA. **(a)** Full spectrum, **(b)** upfield, **(c)** middle field and **(d)** downfield regions. Alanine (1), asparagine (2), glutamine (3), phenylalanine (4), proline (5), tyrosine (6), valine (7), acetic acid (8), citric acid (9), formic acid (10), glyceric acid (11), malic acid (12), malonic acid (13), succinic acid (14), fructose (15), glucose (16), and sucrose (17).

J. Mex. Chem. Soc. **2025**, *69*(3)
Regular Issue

ISSN-e 2594-0317

Table 1. Name, structure and NMR features of the 17 metabolites identified in the aqueous extract of boldo.

No.	Metabolite	Structure	Assignment	δ^{1}H (ppm)	Multiplicity	J (Hz)	δ^{13}C (ppm)
1	Alanine	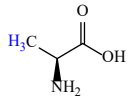	CH_3	1.45	d	9	27.1
2	Asparagine	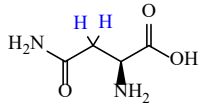	CH_2	2.93	dd	16.9, 4.2	34.8
3	Glutamine	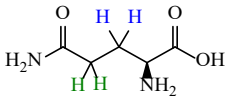	CH_2	2.08-2.17	m		28.6
			CH_2	2.48-2.52	m		35.3
4	Phenylalanine	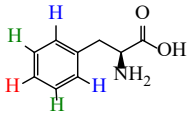	CH	7.31	d	7.5	121.5
			CH	7.38	t	7.5	124.2
			CH	7.43	t	7.5	
5	Proline	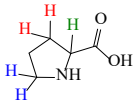	CH	3.33	m		74.1
			CH_2	1.98-2.03	m		23.8
			CH_2	2.07-2.34	m		44.9
6	Tyrosine	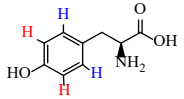	2 CH	7.21	d	7.8	130.7
			2 CH	6.91	d	7.8	116.4
7	Valine	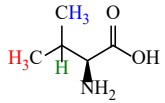	CH_3	0.97	d	7.5	17.2
			CH_3	1.02	d	7.5	23.0
			CH	2.26	m		35.5

J. Mex. Chem. Soc. **2025**, *69*(3)
Regular Issue

ISSN-e 2594-0317

No.	Metabolite	Structure	Assignment	δ^{1}H (ppm)	Multiplicity	J (Hz)	δ^{13}C (ppm)
8	Acetic acid	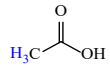	CH_3	1.94	s		23.8
9	Citric acid	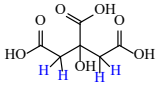	2 CH_2	2.73-2.62	d	15.8	42.1
10	Formic cid		H	8.45	s		159.9
11	Glyceric acid	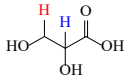	CH	4.09	dd	5.9, 3.1	73.8
			½ CH_2	3.83	dd	5.9, 3.1	62.3
12	Malic acid	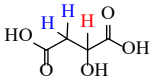	CH_2	2.43-2.71	dd	15.5, 9.6	38.5
			CH	4.32	d	9.6	64.3
13	Malonic acid	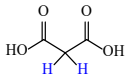	CH_2	3.19	s		47.1
14	Succinic acid	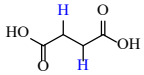	2 CH_2	2.47	s		28.1
15	Fructose	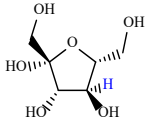	CH	4.11	dd	3.3, 2.4	74.1
			CH	4.02	dd	12.8, 1.4	70.1
			CH	3.56	d	11.6	71.9
			CH_2	3.89-3.70	dd	4.3, 2.4	70.6
			CH_2	3.79-3.71	d	5.6	67.9

J. Mex. Chem. Soc. **2025**, *69*(3)
Regular Issue

ISSN-e 2594-0317

16	α,β-Glucose	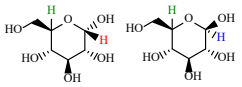	CH	3.24	dd	9.4, 7.9	79.4
			CH	5.23	d	3.7	92.5
			CH	4.63	d	7.9	96.5
			CH	3.41	t	9.4	74.5
			CH	3.40	t	9.6	73.6
			CH	3.49	t	9.2	76.2
17	Sucrose	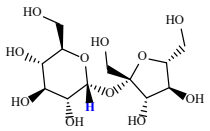	CH	5.51	d	3.8	92.3
			CH	4.21	d	8.8	74.1
			CH	4.05	t	8.8	63.9
			CH	3.76	t	5.8	73.2

J. Mex. Chem. Soc. **2025**, *69*(3)
Regular Issue

ISSN-e 2594-0317

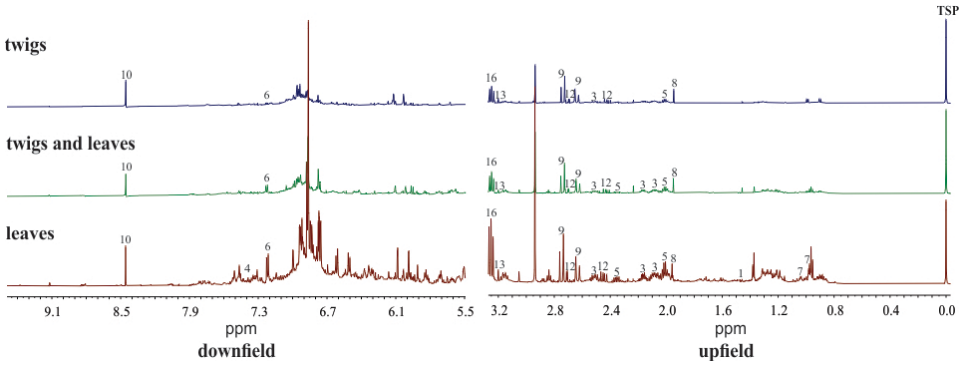

Fig. 3. ^{1}H NMR (600 MHz) of the aqueous extract of boldo twigs, twigs and leaves and only leaves. Alanine (1), glutamine (3), phenylalanine (4), proline (5), tyrosine (6), valine (7), acetic acid (8), citric acid (9), formic acid (10), malic acid (12), malonic acid (13), and glucose (16). All samples were dopped with EDTA.

Statistical multivariate analysis

Principal Component Analysis (PCA) accounted for 89.3 % of the total variance ($R^2X = 0.938$ and $Q^2 = 0.928$). In particular, it showed a clear tendency to separate two main groups: one comprising samples 2 and 4, and the other including samples 1, 3, 5-7. Notably, sample 1 stood out from the second group (Fig. 4**(a)**). This pattern became even more pronounced when supervised Orthogonal Partial Least Squares Discriminant Analysis (OPLS-DA) was applied to the NMR data (Fig. 4**(b)**). In this case, components 1 and 2 accounted for 87.1 % of the total variance ($R^2X = 0.981$, $R^2Y = 0.829$, and $Q^2 = 0.814$).

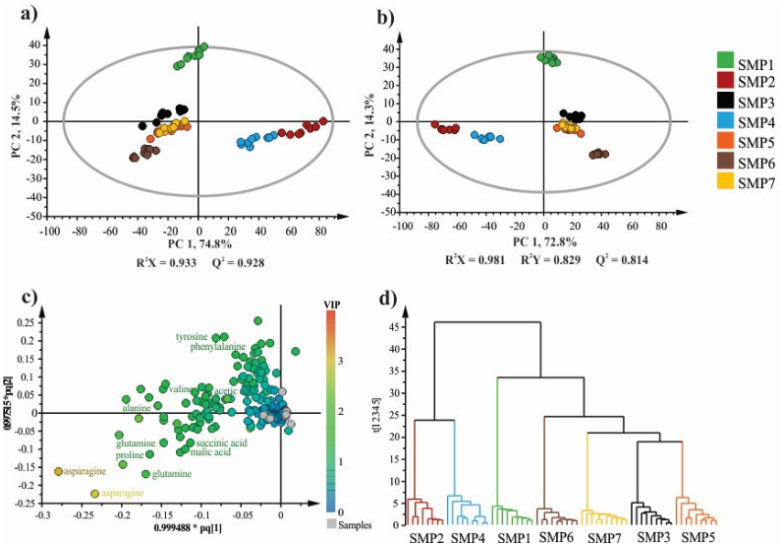

Fig. 4. Multivariate analysis of the infusions of the seven retail samples of *Peumus boldus* leaves. **(a)** PCA and **(b)** OPLS-DA scores plot. **(c)** Loading plot showing metabolites with the most significant influence. **(d)** Hierarchical clustering revealing the grouping between the different boldo tea samples.

The loading plot (Fig. 4**(c)**) and hierarchical clustering (Fig. 4**(d)**) were generated based on the outcomes of the OPLS-DA analysis. The loading plots visually depict the metabolites that exert the greatest discriminatory impact, specifically those that significantly determine the variance of the data. Notably, amino acids such as asparagine, glutamine, proline, alanine, valine, tyrosine, phenylalanine, as well as malic, succinic, and acetic acids where shown to be the metabolites with the highest discriminatory power.

J. Mex. Chem. Soc. **2025**, *69*(3)
Regular Issue

ISSN-e 2594-0317

To quantify their impact, we rely on the Variable Importance in Projection (VIP) scores. Among these, asparagine stands out with a VIP score of 3.10, making the most pronounced contribution to intergroup variance. In contrast, phenylalanine (VIP score: 1.26), exerts a comparatively lower discriminatory effect. The dendrogram depicted in Fig. 4d visually illustrates the hierarchical relationships among sample groups, organized according to their similarities or differences in multivariate data profiles. Within this graphical representation, the initial cluster comprises sample 2 and sample 4, while the second cluster encompasses all remaining samples. As was observed in the scores plot generated from PCA and OPLS-DA (Fig. 4**(a-b)**), within the hierarchical cluster, sample 1 exhibits the highest variance compared to the other samples in its group. Conversely, samples 3, 5 and 7 exhibit the closest similarity to each other within this framework. The validation of the OPLS-DA models was performed by permutation analysis (Fig. S3).

The inner relationship analysis revealed that samples 2 and 6 exhibit the greatest dissimilarity among all samples (Fig. S4). An s-plot derived from the OPLS-DA ($R^2X = 0.998$, $R^2Y = 0.998$ and $Q^2 = 0.996$) analysis of samples 2 and 6 indicated negative correlation in the levels of asparagine (-0.993), alanine (-0.993), glutamine (-0.994), proline (-0.994), and tyrosine (-0.981). Therefore, the concentration of these metabolites decreases between the samples. Conversely, there was a positive correlation with succinic acid (0.730) and formic acid (0.112), leading to an increase in their concentration between the samples.

Quantification of the identified metabolites

Relative quantification was performed using the Chenomx software. Free amino acids play a pivotal role in defining the distinctive flavor and aroma profiles. Among the twenty-six varieties of amino acids identified in the infusion, accounting for the 1 % to 4 % of the plant's dry weight [22], proline (1.42 – 5.68 μM) is the most abundant amino acid in boldo infusion. Conversely, alanine (0.17 – 0.34 μM) and phenylalanine (0.13 – 0.18 μM) exhibit the lowest concentration. Tyrosine (0.29 – 0.60 μM) and valine (0.27 – 0.48 μM) are present in minimal concentrations, while glutamine (1.61 – 3.34 μM) and asparagine (0.85 – 1.86 μM) fall in between as aminoacids of intermediate concentration levels (Fig. 5).

Alanine, arginine, asparagine, aspartic acid, glutamic acid, isoleucine, histidine, leucine, phenylalanine, serine, threonine and tyrosine are the free amino acids found in each infusion [23]. Therefore, the discriminating amino acids defining boldo infusion encompass alanine, asparagine, phenylalanine and tyrosine. These amino acids, crucial for both the flavor profile and health benefits of the infusion, significantly impact its quality [24]. Moreover, they serve as vital precursors, facilitating the generation of aromatic compounds via Maillard reactions, oxidations, and degradation processes [25].

Research has shown that leucine can serve as a precursor in the biosynthesis of other alkaloids. It can transform into the respective aldehyde and then combine with dopamine, thereby leading to the formation of isoquinoline-derived alkaloids [26]. Some amino acids are important precursors of essential metabolites in plants. An example of this is glycosylates, sulfur-rich natural products that, upon conversion by thioglucosidases through hydrolysis, yield compounds as isothiocyanates, thiocyanates, and nitriles. These compounds exhibit anticancer properties or act as pesticides [25] and can be synthesized from branched chain aromatic amino acids, methionine or alanine, which are notably found in boldo infusion [27,10]. Tyrosine arises through the shikimic acid pathway, giving rise to a diverse array of molecular structures such as phenylpropanoids, betalains, catecholamines, tocopherols and others derivates. These compounds hold significant nutritional and pharmacological value [28]. Aspartic acid plays a pivotal role in plants as a precursor of various metabolites, including threonine, leucine and glycine, which are crucial for photorespiratory functions [29].

The most abundant short-chain organic acids are citric (5.04 – 7.91 μM), glyceric (4.59 – 7.80 μM) and malic (2.96 – 5.36 μM) acids, while succinic acid (0.05 – 0.17 μM) is present in lower concentration. Those found in intermediate concentration are malonic (0.81 - 1.16 μM), acetic (0.54 – 1.10 μM) and formic (0.28 – 0.83 μM) acids (Fig. 5). Studies indicate that asparagine can be catabolized to produce malic acid. This process involves converting asparagine to oxosuccinamic acid, which is further reduced to hydroxysuccinamic acid, ultimately leading to the production of malic acid [27]. While malic acid could not be quantified due to signal resolution, it was identified through other NMR experiments.

Glucose (16.09 – 29.76 μM) is the predominant sugar in the metabolome, while sucrose (1.11 – 5.17 μM) stands out as the sugar with the lowest concentration within boldo infusion. Notably, fructose (12.18 – 16.47 μM) exhibits the least variation among samples (Fig. 5). Both glucose and fructose serve as metabolites primarily responsible for fueling diverse energy-dependent processes [21]. In general, the samples to prepare the boldo infusion were those selected based on morphology related to the *Peumus boldus* Molina variety. These

J. Mex. Chem. Soc. **2025**, *69*(3)
Regular Issue

ISSN-e 2594-0317

presented the same metabolomic profile (Fig. 1), whose main difference was found in the relative concentration of metabolites, which may be related to the storage time of the *P. boldus* samples [30].

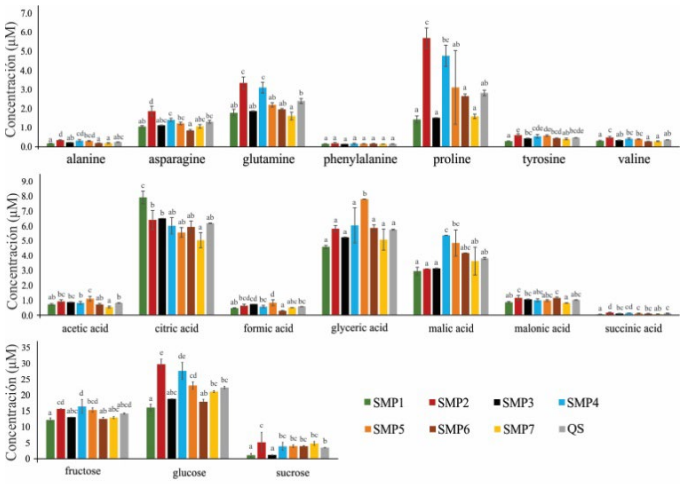

Fig. 5. Relative concentration (µM) of metabolites identified in boldo infusion. Lowercase letters represent the significant differences (ANOVA, p-value ≤ 0.05, ±SD) between different tea brands.

B-plot (Fig. 6) resulted from an OPLS-DA analysis ($R^2X = 0.912$, $R^2Y = 0.672$, and $Q^2 = 0.403$) as outlined in the supplementary materials (Fig. S5), derived from the individual quantification of ^{1}H NMR spectra using the Chenomx software. Samples 1 and 3 exhibit negative correlations with sucrose, glyceric acid, and malic acid, whereas sample 5 shows positive correlations with these metabolites but negative ones with citric acid. On the other hand, samples 6 and 7 demonstrate negative correlations with valine, asparagine, glutamine, proline, phenylalanine, alanine, succinic, malonic, acetic acid, formic acid, glucose, and fructose. In contrast, sample 2 displays positive correlations with the same set of metabolites.

The infusion comprises numerous chemical components, such as amino acids, polyphenols, polysaccharides, volatile oils, vitamins, minerals and alkaloids [26]. Upon examining the correlations among the identified metabolites (Fig. 6), it is observed that the concentration of citric acid rises as the level of sucrose, while malic and glyceric acids decrease. Moreover, tyrosine, glucose, phenylalanine, alanine and glutamine show positive correlation with each other, suggesting a potential connection along the same metabolic pathway or related pathways.

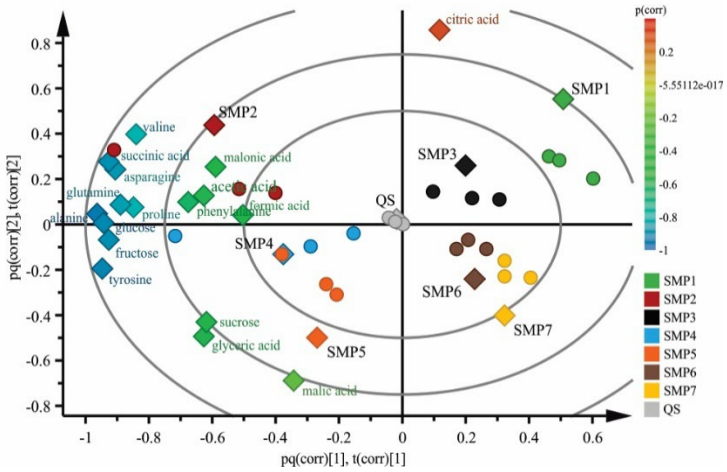

Fig. 6. B-Plot of the quantified metabolites in the boldo infusion metabolome.

J. Mex. Chem. Soc. **2025**, *69*(3)
Regular Issue

ISSN-e 2594-0317

Mass spectrometry analysis

The rising demand for medicinal plants has encouraged their commercialization. Consequently, ensuring the accurate identification of these plants is crucial. Mistaken identity can have severe repercussions, ranging from a lack of the intended therapeutic benefits to potential intoxication. The species *Peumus boldus* Molina are known as true boldo, while *Plectranthus ornatus* [31]*, Plectranthus neochilus* [32], *Plectranthus amboinicus* [33], *Plectranthus barbatus* [34], *Plectranthus grandis* [35], *Plectranthus ornatus* [36], *Vernonia condensate* [37], and *Coleus barbatus* [38] are identified as false boldo. The morphological similarity between these species and the fragmentation of the dried leaves favors the false commercialization of *Peumus boldus* Molina [39]. The marketing of adulterated samples may contain one or more mixed species or even complete substitution of the correct one, thus having a lower antioxidant potential or even health disorders. For instance, *Coleus barbatus* has been used in folk medicine to interrupt pregnancy, delay fetal development and inhibit implantation; indeed, these effects justify its popular use [38]. It is evident the importance to identify biomarkers to detect intentional or mistaken adulterations in medicinal plants available for human consumption.

Boldine is an aporphine alkaloid present in authentic samples of *Peumus boldus* Molina [40]. It is a strong antioxidant with several pharmacological activities, such as anti-inflammatory, antipyretic, antiatherogenic, antiplatelet, antitumor, cytoprotective and tyrosine inhibitor [41]. Although boldine is neither the only nor the most abundant alkaloid in boldo leaves, it is an important biomarker to authenticate *Peumus boldus* Molina [30].

In this sense, a complementary mass spectrometry analysis was carried out with a SolariX Bruker equipment in order to identify boldine or its isomers such as isoboldine, laurotetanine or norisocorydine. Through positive ionization, it was possible to observe the molecular ion corresponding to boldine or boldine isomer in all samples (m/z = 328.15) and *N*-methyllaurotetanine (m/z = 342.17) or its isomer (Norglaucine or Isocorydine) (Fig. S6), it is the main alkaloid present in boldo leaves [30].

Positive ionization results were analyzed using MetaboScape software (2022b), through which another 10 characteristic metabolites of true boldo were identified according to the literature [30, 42, 43]: chlorogenic acid (m/z = 355.08306), coclaurine (m/z = 286.14311), epicatechin (m/z = 291.08672), epicatechin gallate (m/z = 443.17429), laurolitsine (m/z = 314.14603), N-methylcoclaurine (m/z = 300.14712), pronuciferine (m/z = 312.16252), quercetin (m/z = 303.10240) and reticuline (m/z = 330.16861). In negative ionization mode, 11 metabolites characteristic of the authentic boldo plant were identified [43, 44, 45]: 6α,7–dehydroboldine (m/z = 324.13040), bornyl acetate (m/z = 195.04947), caffeic acid (m/z = 179.05491), camphene (m/z = 135.02995), catechin (m/z = 289.07215), chlorogenic acid (m/z = 353.14590), epicatechin (m/z = 289.06862), kaempferol (m/z = 285.07597), p-cymene (m/z = 133.01351), palmitic acid (m/z = 255.22888) and thymol (m/z = 149.04958).

Conclusions

This study represents the first metabolomic analysis by proton nuclear magnetic resonance (^{1}H NMR) of aqueous extracts of seven commercial samples of boldo infusion, conventionally prepared for consumption. It was demonstrated that by knowing the morphology of the plant, it is possible to discard anomalous samples that could alter the desired chemical composition of the infusion. It was found that amino acids and short-chain acids can be used as specific biomarkers to authenticate marketed boldo samples, even to distinguish the presence of plants other than *Peumus boldus* Molina. Mass spectrometry analysis allowed the identification of metabolites characteristic of the authentic plant found in the seven commercial samples studied. Although boldo infusion contains metabolites of relevance for human consumption, further studies on biological activity are needed to establish appropriate intake limits. Despite the significant price differences between the various commercial samples, this protocol allowed us to determine that the samples analyzed have very similar chemical profiles; moreover, it sets an important precedent for the accurate identification of the true boldo metabolome.

Acknowledgments

This research received financial support from Secretaría de Investigación y Posgrado del Instituto Politécnico Nacional-Mexico (SIP-IPN, Mexico) (Grants 20194908, 20210829 and 2022018. **LGZV** thanks

J. Mex. Chem. Soc. **2025**, *69*(3)
Regular Issue

ISSN-e 2594-0317

Programa Institucional de Año Sabático-Instituto Politécnico Nacional (PIAS-IPN) for supporting the completion of this work (February 08, 2021-January 23, 2022). **EBM** thanks Secretaría de Investigación y Posgrado del Instituto Politécnico Nacional-Mexico (SIP-IPN, Mexico) (Grants 20231017). **YNC** thanks to the projects supported by CONACYT: 302670 in the 2019 call for support for the acquisition and maintenance of infrastructure in institutions and specialized research laboratories, CF-2019/6669 in the frontier science call. **EJTS** thanks CONAHCYT for the scholarship awarded during her doctoral studies. (CVU 773263).

References

1. Ravindran, P.N.; Pillai G.S.; Divakaran M. K.V. *Peter.Woodhead Publishing*. **2012**, *2*, 557-582. DOI: https://doi.org/10.1533/9780857095688.557.
2. Cassels, B. K. *Springer, Cham.* **2021**, *2*, 429-438. DOI: https://doi.org/10.1007/978-3-030-62818-5_33.
3. Vogel, H.; Razmilic, I.; Muñoz, M.; Doll, U.; San Martín, J. *Planta Med*. **1999**, *65*, 90-91. DOI: https://doi.org/10.1055/s-2006-960450.
4. Speisky, H.; Cassels, B.K. *Pharmacol. Res.* **1994**, *29*, 1-12. DOI: https://doi.org/10.1016/1043-6618(94)80093-6.
5. De Souza, P.; Vilhena da Silva, R.; Mota da Silva, L.; Steimbach, V.; Moreno, K.; Gasparotto, A. *J. Evidence-Based Complementary Altern. Med.* **2022**, *2022*, 4560607. DOI: https://doi.org/10.1155/2022/4560607.
6. Refaie, A.; Shalby, A. B.; Booles H. F.; Kassem, S.M.; Eshak, M. G.; Farrag, A.R.H.; Khalil W.K.B. *Egypt. J. Chem.* **2022**, *65*, 687-698. DOI: https://doi.org/10.21608/EJCHEM.2022.120306.5401.
7. O'Brien, P.; Carrasco-Pozo, C.; Speisky, H. *Chem. Biol. Interact*. **2006**, *159*, 1-17. DOI: https://doi.org/10.1016/j.cbi.2005.09.002.
8. Yang, X.; Gao, X.; Cao, Guo, Q.; Li, S.; Zhu, Z.; Zhao, Y.; Tu, P.; Chai, X. *Planta Med*. **2018**, *84*, 20-25. DOI: https://doi.org/10.1055/s-0043-113447.
9. Subramaniam, N.; Kannan, P.; Ashokkumar K.; Thiruvengadam, D. *J. Biochem. Mol. Toxicol*. **2019**, *33*, e22404. DOI: https://doi.org/10.1002/jbt.22404.
10. Heidari, R.; Moezi, L.; Asadi, B.; Ommati, M.M.; Azarpira, N. *PharmaNutrition*. **2017**, *5*, 109-117. DOI: https://doi.org/10.1016/j.phanu.2017.07.001.
11. Park, I; Lee, H-S; Lee, S-G; Park, J-D; Ahn, V-J. *J. Econ. Entomol.* **2000**, *93*, 331-335. DOI: https://doi.org/10.1603/0022-0493-93.2.331.
12. Otero, C.; Miranda-Rojas, S.; Llancalahuén, F.M.; Fuentes, J.A.; Atala, C.; González-Silva, G.; Verdugo, D.; Sierra-Rosales, P., Moreno, A., Gordillo-Fuenzalida, *F. Food Chem.* **2022**, *370*, 131012. DOI: https://doi.org/10.1016/j.foodchem.2021.131012.
13. Passone, M.A; Etcheverry, M. *Int. J. Food Microbiol*. **2014**, *168-169*, 17-23. DOI: https://doi.org/10.1016/j.ijfoodmicro.2013.10.009.
14. Silva Borges de Castro, D.; Brentan da Silva, D.; Domingues-Tibúrcio, J.; Guerra-Sobral, M.E.; Ferraz, V.; Gutterres-Taranto, A.; Serrão, J.E.; Máximo de Siquiera, J.; Nunes-Alves, S. *Exp. Parasitol*. **2016**, *171*, 84-90. DOI: https://doi.org/10.1016/j.exppara.2016.10.008.
15. Dias-Machado, C.; Pereira dos Santos, V.L.; Schimandeiro-Novak, R., Schechtel-Koch, M., Arcaro, G., Raman, V., Cavichiolo-Franco, C.R., Farago, P.V., Manfron-Budel, J. *Flora*. **2021**, *279*, 151827. DOI: https://doi.org/10.1016/j.flora.2021.151827.
16. Cardoso-Correla-Teixeira, C.; Pereira de Freitas-Carbal, T.; Barreto de Sousa, J.P., Teixeira, S.P.; Kenupp-Bastos, J.; de Freitas, L.A.P. *Pharmacogn. J.* **2016**, *8*, 264-272. DOI: https://doi.org/10.5530/pj.2016.3.16.
17. Steenkamp, P.A; Steenkamp, L.H.; Mancama, D.T. *Springer, Cham*. **2018**, 303-347. DOI: https://doi.org/10.1007/978-3-319-62229-3_10.

J. Mex. Chem. Soc. **2025**, *69*(3)
Regular Issue

ISSN-e 2594-0317

18. Félix-Silva, J.; Tomaz, I.M.; Silva, M.G.; Santos, K.S.C.R.; Silva-Júnior, A.A.; Carvalho, M.C.R.D.; Soares, L.A.L.; Fernandes-Pedrosa, M.F. *Rev. Bras. de Plantas Medicinais.* **2012**, *14*, 548-555. DOI: https://doi.org/10.1590/S1516-05722012000300018.
19. Bakiri, A.; Hubert, J.; Reynaud, R.; Lanthony, S.; Harakat, D.; Renault, J-H.; Nuzillard, J-M. *J. Nat. Prod.* **2017**, *80*, 1387-1396. DOI: https://doi.org/10.1021/acs.jnatprod.6b01063.
20. Simirgiotis, M.J.; Schmeda-Hirschmann, G. *J. Chromatogr. A.* **2010**, *1217*, 443-449. https://doi.org/10.1016/j.chroma.2009.11.014.
21. Torres-Vega, J; Gómez-Alonso, S; Pérez-Navarro, J; Pastene-Navarrete, E. *Plants*. **2020**, *9*, 242 DOI: https://doi.org/10.3390/plants9020242.
22. Xu, Y; Liu, Z; Liu, Z; Feng, Z; Zhang, L; Wan, X; Yang, X. *Food Chem.* **2020**, *317*,126428. DOI: http://doi.org/10.1016/j.foodchem.2020.126428.
23. Zhao, M.; Ma, Y; Dai, L-L; Zhang, D-L; Li, J-H; Yuan, W-X; Li, Y; Zhou, H. *Food Anal. Methods.* **2013**, 6(1), 69–75. DOI: https://doi.org/10.1007/s12161-012-9408-4.
24. Alcázar, A; Ballesteros, O; Jurado, J. M; Pablos, F; Martín, M. J; Vilches, J. L; Navalón, A. *J. Agric. Food Chem.* **2007**, *55*, 5960-5965. DOI: https://doi.org/10.1021/jf070601a.
25. Gladden, L. B. *J. Physiol.* **2004**, *558*, 5-30. DOI: https://doi.org/10.1113/jphysiol.2003.058701.
26. Seigler, D.S.S. *Plant Secondary Metabolism.* **1998**, 578–616. DOI: https://doi.org/10.1007/978-1-4615-4913-0_32.
27. Lea, P.J.; Sodek, L.; Parry, M.A.J.; Shewry P.R.; Halford, N.G. *Ann. Appl. Biol.* **2006**, *150*, 1-26. https://doi.org/10.1111/j.1744-7348.2006.00104.x.
28. Asai, N; Nakajima, N; Tamaoki, M; Kamada, H; Kondo, N. *Plant Cell Physiol*. **2000**, *41*, 10-15. DOI: https://doi.org/10.1093/pcp/41.1.10.
29. Kirma, M; Araújo, W. L; Fernie, A. R; Galili, G. *J. Exp. Bot*. **2012**, *63*, 4995-5001. https://doi.org/10.1093/jxb/ers119.
30. Fuentes-Barros, G; Castro-Saavedra, S; Liberona, L; Acevedo-Fuentes, W; Tirapegui, C; Mattar, C; Cassels, B. K. *Fitoterapia.* **2018**, *127*, 179–185. DOI: https://doi.org/10.1016/j.fitote.2018.02.020.
31. Ribeiro, F. F; Da Conceicão, L.D.O; Oyama, E. M; Furlan, M. R. *Visão Acadêmica*. **2017**, *18*. DOI: https://doi.org/10.5380/acd.v18i3.54224.
32. Santos, R.L.; Nobre, M.S.C., Guimarães, G.P., Viera, K.V.M., Felismino, D.C., Dantas, I.C., Silva, L.A. *CABI*, **2011**, *9781845938338.0666*, 666-669. DOI: https://doi.org/10.1079/9781845938338.0666.
33. Mauro, C; Silva, C. de P; Missima, J; Ohnuki, T; Rinaldi, R. B; Frota, M. *Rev. Brasileira de Farmacognosia*. **2008**, *18*, 608–613. DOI: https://doi.org/10.1590/s0102-695x2008000400019.
34. Pereira-Dos Santos, L; Azevedo-Martins, R.C.; Kelce-Pires, C; Oliveira-Gomes, A; Larcher-De Almeida, M.F; Cruz-Da Rocha, E.D.A; Santana-Carvalho, E.L; Dolejal-Zanetti, G. *Braz. J. Health Rev.* **2023**, *6*, DOI: https://doi.org/10.34119/bjhrv6n2-059.
35. Milaneze-Gutierre, M. A; Famelli, M. C; Capel, L. S; Romagnolo, M. B. *Acta Sci.Biol. Sci.* **2007**, *29*, 125-130.
36. Ramos da Silva, L.R.; Ataide-Correia, Z; Cajueiro-Gurgel, E.S; Ribeiro, O; Gomes-Silva, S; Oliveira-Ferreira, O; Andrade, E.H.A; Santana de Oliveira, M. *Molecules*. **2023**, *28*, 6482. DOI: https://doi.org/10.3390/molecules28186482.
37. Duarte, M. D. R.; Lopes, J. F. *Rev. Brazilian Pharmacogn*. **2007**, *17*, 549-556. DOI: https://doi.org/10.1590/S0102-695X2007000400013.
38. Almeida, F. C. G.; Lemonica, I. P. *J. Ethnopharmacol*. **2000**, *73*, 53–60. DOI: https://doi.org/10.1016/s0378-8741(00)00275-0.
39. Machado, C. D; Pereira dos Santos, V. L; Novak, R. S; Koch, M. S; Arcaro, G; Raman, V; Budel, J. M. *Flora.* **2021**, *279*, 151827. DOI: https://doi.org/10.1016/j.flora.2021.151827.

J. Mex. Chem. Soc. **2025**, *69*(3)
Regular Issue

ISSN-e 2594-0317

40. Kazemi-Noureini, S; Tanavar, F. *Chem.-Biol. Interact.* **2015**, *231*, 27–34. DOI: https://doi.org/10.1016/j.cbi.2015.02.020.
41. Siiang-Lau, Y; Chih-Ling, W; Murugan, D; Mustafa, M.R. *J. Cardiovasc. Pharmacol*. **2015**, *65*, 522-531. DOI: https://doi.org/10.1097/FJC.0000000000000185.
42. Cassels, B.K.; Fuentes-Barros, G.; Castro-Saavedra, S. *Curr. Tradit. Med.* **2018**, *5*, 31-65. DOI: https://doi.org/10.2174/2215083804666181113112928.
43. Galvez-Ranilla, L.; Knon, Y.I.; Apostolidis, E.; Shetty, K. *Bioresour. Technol.* **2010**, *10*, 4676-4689. DOI: https://doi.org/10.1016/j.biortech.2010.01.093.
44. Mello de Souza, W.F.; Mariano, X.M.; Isnard, J.L.; Santos de Souza, G.; De Souza, A.L.; Tavares de Carvalho, R.J.; Barbosa, C.; Siqueira, C.L.; Alves, R.F. *Food Int. Res.* **2019**, *124*, 27-33. DOI: https://doi.org/10.1016/j.foodres.2018.12.059.
45. Simirgiotis, M.J.; Schemeda-Hirschmann, G.J. *Chromatogr. A.* **2010**, *1217*, 443-449. DOI: https://doi.org/10.1016/j.chroma.2009.11.014.